·Experimental Research·

The therapeutic effect and mechanism of small extracellular vesicles derived from mesenchymal stem cells (MSCs) on retinal light injury

Yu Bo[1], Wang Kang[2], Zhang Mingliang[1], Xing Xiaoli[1], Li Xiaorong[1], Zhang Xiaomin[1]

[1]Tianjin Key Laboratory of Retinal Functions and Diseases, Tianjin Branch of National Clinical Research Center for Ocular Disease, Eye institute and School of Optometry, Tianjin Medical University Eye Hospital, Tianjin 300384, China; [2]Department of ophthalmology, Binzhou Medical University Hospital, Binzhou 256600, China

Corresponding author: Zhang Xiaomin, Email: xzhang08@tmu.edu.cn

[Abstract] Objective To investigate the effect of small extracellular vesicles (sEVs) derived from mesenchymal stem cells (MSCs) in mouse model of retinal light injury and the possible mechanism.

Methods Human umbilical cord derived MSCs were identified by flow cytometry. Supernatants of passage 3-5 MSCs were collected. sEVs were harvested by ultracentrifugation and were identified by transmission electron microscopy. Sixty-five healthy female specific pathogen free (SPF)-grade BALB/c mice aged 8-10 weeks were randomly divided into normal group (17 mice), phosphate buffered saline (PBS) group (24 mice) and sEVs group (24 mice). Mice in PBS and sEVs groups were intravitreally injected with 2 μl of PBS and sEVs, respectively, and were exposed to 930 lx blue light for 6 hours. No intervention was administered to the normal group. Three days after lighting, mice retinal structure was observed by hematoxylin-eosin staining. Apoptotic retinal cells were detected by terminal deoxynucleotidyl transferase-mediated dUTP nick-end labeling (TUNEL). Retinal function was tested by electroretinogram. Differentially expressed mRNAs between PBS group and sEVs group were assayed by mRNA transcriptome sequencing and were analyzed through KEGG cluster analysis. The differential mRNAs were verified via real-time quantitative PCR. The study protocol was approved by the Animal Ethics Committee of Tianjin Medical University Eye Hospital (No.TJYY20201221035).

Results MSCs were positive for CD90 and CD105, negative for CD34 and CD45.The extracted MSC-sEVs showed a bilayer membrane vesicle with a diameter of 80-140 nm. Hematoxylin-eosin staining showed the arrangement of photoreceptor nuclei was disordered in outer nuclear layer in PBS group. The disorder of photoreceptor nuclei arrangement of sEVs group was slighter than that of PBS group. The apoptotic cell number of sEVs group was (14.60±4.04)/visual field, which was lower than (24.00±8.52)/visual field of PBS group, with a statistically significant difference (t=2.37, P<0.05). The a-wave amplitude of sEVs group was (64.38±16.70)μV, which was higher than (16.78±6.37) μV of PBS group, showing a statistically significant difference (P<0.05). The b-wave amplitudes of PBS and sEVs groups were (132.40±39.41)μV and (154.86±34.08)μV, respectively, which were lower than (338.38±27.41) μV of normal group, and the differences were statistically significant (both at P<0.05). A total of 110 differentially expressed mRNAs were detected. There were 109 downregulated mRNAs in sEVs group. Differentially expressed mRNAs were mainly inflammation- and immune-related pathways. PCR showed that the expression level of C-C motif chemokine ligand 2, C-C motif chemokine receptor 2, leukotriene B4, leukocyte Ig-like receptor A6 and interleukin-1β in sEVs group were significantly decreased in comparison with PBS group (all at P<0.05).

Conclusions MSC-sEVs can ameliorate blue light-induced retinal structural and functional damage. The protective effect may be achieved through inhibiting inflammatory response.

[**Key words**] Retina; Light injury; Mesenchymal stem cell; Small extracellular vesicle

Fund program: National Natural Science Foundation of China (81800825); Tianjin Natural Science Foundation (21JCQNJC01630); Open Project of Tianjin Key Laboratory of Retinal Functions and Diseases (2021tjswmq002)

DOI: 10.3760/cma.j.cn115989-20220412-00157

Blue light irradiation causes photochemical damage to the retina, resulting in oxidative stress damage and functional decline of photoreceptors, which will eventually lead to degeneration, apoptosis, and necrosis of photoreceptors. The pathological process of retinal light injury is similar to that of photoreceptor injury in retinal degenerative diseases [1]. Thus, a mouse retinal light injury model is commonly used to study photoreceptor injury and retinal degenerative diseases. Antioxidants [phenyl-N-tert-butyl nitrone, saffron] have been shown to play a neuroprotective role in retinal injury animal models [2-3]. Topical injection of ciliary neurotrophic factor (CNTF) can reduce photoreceptor degeneration and protect retinal function [4]. In addition, gene therapy has also been shown to play a neuroprotective role in treatment for neurodegeneration in a mouse retinal degeneration model [5]. Prevention is currently the most common management for retinal degeneration diseases and retinal injuries. However, no effective treatment has been developed to rescue degeneration or apoptosis of neurons. It has been shown that small extracellular vesicles (sEVs) derived from mesenchymal stem cells (MSCs) have similar biological functions as MSCs, such as anti-inflammatory, neuroprotective, immune regulative, and tissue reparative effects [6-8]. MSC-sEVs have been reported to play therapeutic roles in animal models of uveitis, corneal transplantation rejection, retinal detachment, and retinal laser injury [9]. However, their application in a retinal light injury model has not been reported. In the current study, the protective effect of MSC-sEVs on retinal injury and its possible mechanism were studied in a mouse retinal light injury model, providing an experimental basis for retinal neuroprotective treatments.

1 Materials & Methods

1.1 Materials

1.1.1 Histogenesis of MSCs MSCs were purchased from Beilai Biotechnology (Beijing, China).

1.1.2 Animals Sixty-five SPF-grade healthy female BALB/c mice (age range: 8-10 weeks) with body weights of 18-20 g were purchased from Weitong Lihua Experimental Animal Technology (Beijing, China). Clear refractive media were guaranteed in each mouse. The care and use of animals conformed to the Regulations for the Administration of Affairs Concerning Experimental Animals issued by The State Science & Technology Commission. Animals were housed in an SPF laboratory animal room, at a temperature of (23±2)℃, humidity of 55%±10%, and 12-hour light/12-hour dark cycles. The current study was approved by the Animal Ethics Committee of Tianjin Medical University Eye Hospital (TJYY20201221035).

1.1.3 Reagents and Instruments The reagents and instruments were used were as follows: a universal RNA purification Kit (EZB-RN4, EZBioscience, Roseville, MN, USA), color reverse transcription kit (EZB-A0010CGQ; EZBioscience), *in situ* cell death detection kit (Roche, Basel, Switzerland), FACSCalibur flow cytometer (BD Biosciences, San Jose, CA, USA), CM10 transmission electron microscope (Phillips Electron Optics, Eindhoven, The Netherlands), BX51 optical microscope (Olympus, Tokyo, Japan), and Ganzfeld scotopic electroretinogram instrument (Phoenix Research Labs, Plesanton, CA, USA).

1.2 Methods

1.2.1 MSC culture and identification and MSC-sEV collection Third generation MSCs were cultured in an incubator at 37 ℃ with 5% CO_2. The medium was changed every 2−3 days according to the condition of cell growth. MSCs were passaged when they reached 80% confluency and from passage 3 to 5, MSCs were cultured in exosome-free conditioned medium. Supernatants of MSCs at passages 3−5 were collected and centrifuged at 300 × *g* for 10 minutes, 2,000 × *g* for 20 minutes, 10,000 × *g* for 30 minutes, and 110,000 × *g* for 70 minutes, twice. The precipitates were resuspended in phosphate-buffered saline (PBS) to a protein concentration of 0.5 g/L and were filtered through a 0.22 μm membrane filter. The surface markers of MSCs (CD90, CD105, CD34, and CD43) were analyzed by flow cytometry as described methods in reference [10]. Morphological characteristics and ultrastructure of MSC-sEVs were examined using a transmission electron microscopy (TEM).

1.2.2 Establishment of the retinal light injury animal model and animal grouping Animals were divided into a normal group (17 mice), PBS group (24 mice), and sEV group (24 mice) using a randomized number table. Pupils of right eyes were dilated with 1% atropine sulfate, and 2 μl PBS or 0.5 g/L sEVs were intravitreally injected. Mice were exposed to (930±5) lux of blue light, in cages. Single mice were caged to avoid shielding of the light. The normal group mice received no treatment. Three days after treatment, experiments were conducted using mice in the PBS and sEV groups.

1.2.3 Hemoxylin & eosin (HE) staining for retinal structures analysis Five mice from each group were selected using a randomized number table. Mice were sacrificed by cervical dislocation, and the right eyes were enucleated. Eyes were first dehydrated in a series of ethanol solutions with different concentrations (70%, 80%, 90%, 100%, and 100%), each for 40 min. Then, after being soaked in xylene, they were embedded in paraffin. Eyes were then sectioned near or through the optic nerve at 4 μm thicknesses, soaked in xylene, immersed in gradient ethanol solutions, stained with HE, and observed and photographed using an optical microscope.

1.2.4 TUNEL staining for the detect of apoptosis of retinal cells One mouse from the normal group, five mice from the PBS group, and five mice from the sEV group were selected using a randomized number table. Mice were sacrificed by cervical dislocation, and the right eyes were enucleated. Paraffin sections were made according to the methods described in 1.2.3. TUNEL staining was performed as follows according to the manufacturer's instructions of the *in situ* cell death detection kit. Sections were soaked in xylene, immersed in gradient ethanol solutions, permeabilized with Triton X-100 in 0.1% sodium citrate for 10 min, rinsed in PBS, and incubated in a humidified chamber for 60 min at 37 ℃ after fluorescent reagents were added. Sections were then stained with 4',6-diamidino-2-phenylindole and sealed with anti-fluorescence quencher. Apoptotic cells were observed and counted using a fluorescence microscope. For each section, three discontinuous visual fields were randomly examined, and apoptotic cells were counted and averaged.

1.2.5 Electroretinography (ERG) record for the assessment of retinal function Five mice from each group were selected using a randomized number table. After dark-adaption for 16 h, the mice were anesthetized by intraperitoneal injection of a tiletamine hydrochloride and zolazepam hydrochloride (1:1) mixture at a concentration of 65 mg/kg and xylazine hydrochloride at a concentration of 10 mg/kg. Pupils of right eyes were dilated by compound tropicamide eye drops, and the corneal surface was anesthetized with 0.5% proparacaine HCI eye drops. Deproteinized calf blood extract eye gel (Shenyang Xingqi Pharmaceutical CO.LTD, China) was applied and a platinum electrode was placed in the cornea. The reference and ground electrodes were placed subcutaneously in the head and tail, respectively. Ganzfeld scotopic electroretinogram instrument (Phoenix Research Labs, Plesanton, CA, USA) was used to record a Ganzfeld scotopic ERG for retinal functional assessment under a white light flash with intensity of 3.1 log cd•s/m^2 [11], and a wave and b wave amplitudes were then observed and compared.

1.2.6 Transcriptome sequencing and analysis of differential mRNA expression Three mice from each group were selected using a randomized number table. Mice were sacrificed by cervical dislocation, and the right eyes were enucleated. The cornea was cut-off along the limbus and the lens was removed. Retina tissues were placed immediately in liquid nitrogen and stored in a -80 ℃ freezer. The mRNA extraction and sequencing were performed by BGI Genomics (Copenhagen, Denmark). Differentially expressed genes (fold-change > 2, Q-value < 0.05) were screened and Kyoto Encyclopedia of Genes and Genomes (KEGG) cluster analysis was performed.

1.2.7 Real-time fluorescence PCR for verification of differentially expressed mRNA The remaining six mice from the PBS and sEVs groups were sacrificed by cervical dislocation, and the right eyes were enucleated. Retinal tissues were dissociated, total RNA was extracted using an RNA extraction kit [EZB-RN4],

and cDNA was synthesized using a cDNA synthesis kit [EZB-A0010CGQ, EZBioscience Company, Roseville, MN55113, the United States]. Primers of C-C motif chemokine ligand 2 (CCL2), C-C motif chemokine receptor 2 (CCR2), leukotriene (LTB4), C-type lectin domain family (CLEC4D), leukocyte Ig-like receptor (LILRA6), S100 calcium binding protein (S100A9), CD300 molecule-like family member B (CD300LB), schlafen 1 (SLFN1), and interleukin-1β (IL-1β) cDNA, and SYBR were mixed in wells of 384-well plates. The reaction system final volume was 10 μL. PCR amplification conditions were 5 minutes at 95°C, 40 cycles at 95 °C for 10 s, and 60 °C for 30 s. *GAPDH* was used as the internal reference gene. The relative mRNA levels were calculated using the $2^{-\triangle\triangle Ct}$ method. Samples were run in duplicate. Each experiment was repeated three times, and the average value was taken. Forward and reverse primer sequences are listed in Table 1.

Table 1 Primer sequences of target genes

Primers	Sequences	Product length (bp)
GAPDH	forward: 5′-TGTGTCCGTCGTGGATCTGA-3′ reverse: 5′-CCTGCTTCACCACCTTCTTGA-3′	77
CCL2	forward: 5′-CAGGTCCCTGTCATGCTTCTG-3′ reverse: 5′-GAGCCAACACGTGGATGCT-3′	67
CCR2	forward: 5′-ATCCACGGCATACTATCAACATC-3′ reverse: 5′-CAAGGCTCACCATCATCGTAG-3′	104
LTB4	forward: 5′-ATGGCTGCAAACACTACATCTC-3′ reverse: 5′-GACCGTGCGTTTCTGCATC-3′	162
CLEC4D	forward: 5′-ACCCGACATCCCCAACTGAT-3′ reverse: 5′-CTCTCGTCCAGCGTAAAAAGT-3′	118
LILRA6	forward: 5′-CCCTGGTGCTAGTAGTGACAG-3′ reverse: 5′-GTGATAGCTCTGCGAAGACTC-3′	119
S100A9	forward: 5′-ATACTCTAGGAAGGAAGGACACC-3′ reverse: 5′-TCCATGATGTCATTTATGAGGGC-3′	129
CD300LB	forward: 5′-TGCAGGGTCCTCATCCGAT-3′ reverse: 5′-TGTCCGTGTCATTTTGCCTGA-3′	130
SLFN1	forward: 5′-CTAAATGCAGGAGGGATCACAC-3′ reverse: 5′-GAGCACACAGAGCTTTTGTAATG-3′	103
IL-1β	forward: 5′ - GCAACTGTTCCTGAACTCAACT-3′ reverse: 5′-ATCTTTTGGGGTCCGTCAACT-3′	89

Note: CCL: C-C motif chemokine; CCR: C-C motif chemokine receptor; LTB4: leukotriene B4; CLEC4D: C-type lectin domain family 4D; LILRA6: leukocyte Ig-like receptor A6; S100A9: S100 calcium binding protein A9; CD300LB: CD300 antigen-like family member B; SLFN1: schlafen 1; IL: interleukin

1.3 Statistical analysis

Statistical analysis was performed using SPSS statistical software for Windows, version 25.0 (SPSS, Chicago, IL, USA). Histograms showed that the metrological data were close to normal distribution. Results are expressed as $\bar{x}\pm s$. Differences between two groups were compared using independent *t*-tests. One-way analysis of variance was performed for comparisons of three groups. Comparisons between groups were made using Tukey's test. A value of $P<0.05$ was considered statistically significant using two-tailed tests.

2 Results

2.1 Identification of MSCs and MSC-sEVs

The results of flow cytometry showed that cultured MSCs were both CD90 and CD105 positive, whereas CD34 and CD45 were negative (Figure 1A-D). MSCs at 3 days after the first passage were spindle-shaped with a closed whirl-pool-like arrangement when viewed using an optical microscope, which met the requirements of MSC identification (Figure 1E). MSC-sEVs showed a circular vesicle structure with diameters of 80-140 nm using a transmission electron microscope (Figure 1F).

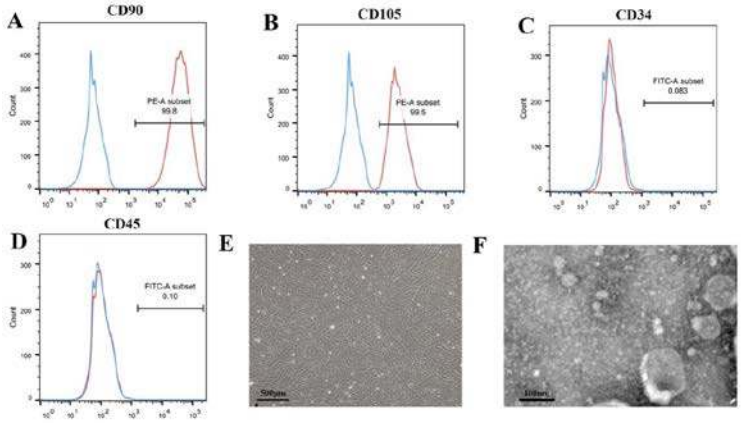

Figure 1 Identification of mesenchymal stem cells (MSCs) and MSC-small extracellular vesicles (sEVs) A: Flow cytometry showed that 99.8% of MSCs were CD90-positive B: Flow cytometry showed that 99.5% of MSCs were CD105-positive C: Flow cytometry showed that very few MSCs were CD34-positive D: Flow cytometry showed that few MSCs were CD45-positive E: Passage 1, MSCs were spindle-shaped and adherent, using a light microscope (×400, bar=500 μm) F: MSC-sEVs showed circular vesicle structures with diameters of 80-140 nm, using a transmission electron microscope (×12 000, bar=100 nm)

2.2 Retina histopathology of each group

Retinal structure was complete with orderly cell arrangement in the normal group (Figure 2A). Photoreceptor nuclei and the outer segments were sparse and disordered in arrangement in the PBS group (Figure 2B). Retinal structures of the sEV group showed morphological changes that resembled those found in the PBS group, but to a lesser extent (Figure 2C).

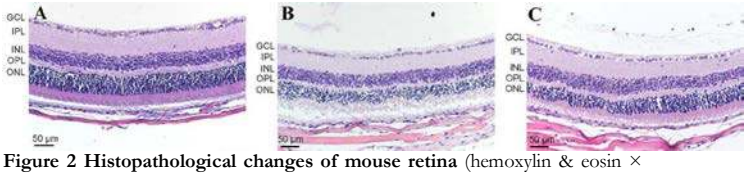

Figure 2 Histopathological changes of mouse retina (hemoxylin & eosin × 200, bar=50 μm) A: In the normal group, retinal structure was intact with an orderly cell arrangement B: In the PBS group, photoreceptor nuclei and cell outer segments were sparse and the arrangement were disordered C: In the sEV group, retinal structural damage was less severe when compared with the PBS group GCL: ganglion cell layer; IPL: inner plexiform layer; INL: inner nuclear layer; OPL outer plexiform layer; ONL: outer nuclear layer

2.3 Comparison of retinal apoptotic cells between two groups

A large number of apoptotic cells were found in the outer nuclear layer and appeared a green fluorescence (Figure 3A, B). The number of apoptotic cells was (14.60±4.04/field) in the sEV group, which was significantly less than 24.00±8.52/ field in the PBS group. The difference was statistically significant ($t=2.37$, $P<0.05$; Figure 3C).

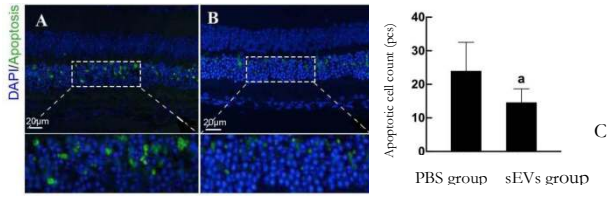

Figure 3 TUNEL staining and apoptotic cells in mouse retina (× 400, bar=20 μm) **A**poptotic cells presented green fluorescence (FITC), and the cell nuclei showed the blue fluorescence (DAPI) A: A large number of were observed in retinal outer nuclear layer in the PBS group B: A small number of apoptotic cells were observed in retinal outer nuclear layer in the sEV group C: Comparison of apoptotic cell counting between the two groups Compared with the PBS group, $^aP<0.05$ (independent samples *t* test, $n=5$) PBS: phosphate-buffered saline; sEV: small extracellular vesicle

2.4 Retinal functional changes in different groups

The a-wave amplitudes were (193.20±12.50), (16.78±6.37), and (64.38±16.70) μV in the normal, PBS, and sEVs groups, respectively, showing a significant difference among three groups ($F=262.70$,

P<0.05), and the a-wave amplitude was significantly elevated in the sEVs group compared with the PBS group (*P*<0.05). The b-wave amplitudes were (338.38±27.41), (132.40±39.41), and (154.86±34.08) μV in the normal, PBS, and sEVs groups, respectively, showing a significant difference among three groups (*F*=55.26, *P*<0.05), and b-wave amplitude in the sEV group was significantly higher than that in the PBS group (*P*<0.05; Figure 4).

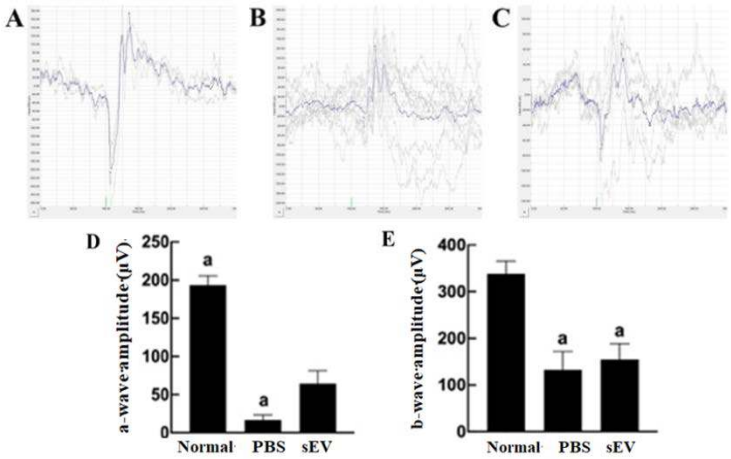

Figure 4 Comparison of a- and b-wave amplitudes of scotopic electroretinograms (ERGs) among three groups A: The scotopic ERG wave pattern of the normal group B: The scotopic ERG wave pattern of the PBS group C: The scotopic ERG wave pattern of the sEV group. D: Comparison of a-wave amplitudes among the three groups *F*=262.70, *P*<0.05. Compared with the sEV group, [a]*P*<0.05 (One-way analysis of variance, Tukey's test, *n*=5) E: Comparison of b-wave amplitudes among the three groups (*F*=55.26, *P*<0.05). Compared with the sEV group, [a]*P*<0.05 (One-way analysis of variance, Tukey test, *n*=5) PBS: phosphate-buffered saline; sEV: small extracellular vesicle

2.5 Analysis of differentially expressed genes and their functional pathways in mouse retinas of the PBS and sEV groups

The mRNA transcriptome sequencing results showed that 110 genes were differentially expressed when comparing the PBS and sEV groups, among which 109 genes were down-regulated and one gene was up-regulated in the sEV group, when compared with the PBS group (Figure 5A). KEGG cluster analysis showed that the differential genes were mainly involved in inflammatory and immune-related signaling pathways. Among the top 10 genes from the differential fold ranking, signaling pathways relevant to retinal damage included natural killer cell-mediated cytotoxicity, B cell receptor signaling, chemokine signaling, leukocyte transendothelial migration, and phagocytosis pathways (Figure 5B).

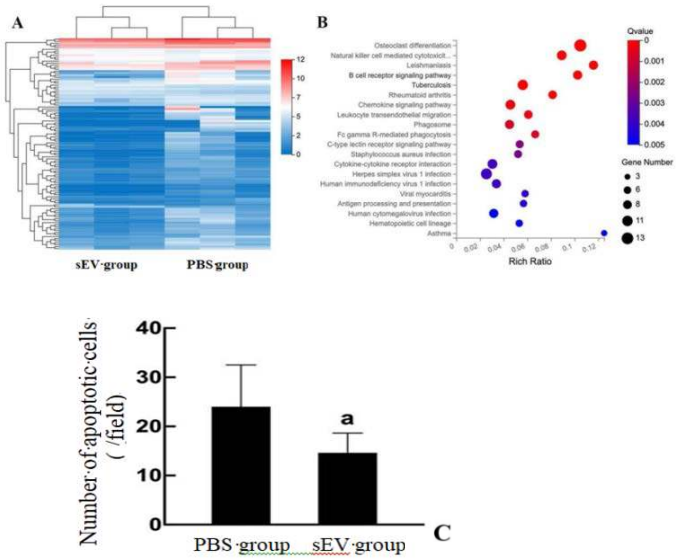

Figure 5 The mRNA transcriptome sequencing and Kyoto Encyclopedia of Genes and Genomes (KEGG) analysis of differentially expressed genes A: Heat map of differentially expressed genes between the sEV and PBS groups B: KEGG cluster analysis of differentially expressed genes PBS: phosphate-buffered saline; sEV: small extracellular vesicle; PBS: phosphate-buffered saline

2.6 Comparison of CCL2, CCR2, LTB4, CLEC4D, LILRA6, S100A9, CD300LB, SLFN1, and IL-1β mRNA expressions in each group

Relative expressions of CCL2, CCR2, LTB4, LILRA6, IL-1 β, CLEC4D, S100A9, and SLFN1 mRNA were significantly different among the normal, PBS, and sEV groups (*F*=92.49, 45.49, 104.10, 80.32, 40.44, 31.16, 12.95, and 21.89, respectively, all *P*<0.05). However, there was no significant difference in the mRNA relative expressions of CLEC4D, S100A9, and SLFN1 between the PBS and sEV groups (all *P*>0.05). In addition, there was no significant difference in mRNA relative expressions of CD300LB among three group (*F*=1.60, *P*>0.05, Table 2).

Table 2 Comparison of mRNA relative expression levels of retinal differential genes among three groups ($\bar{x}\pm s$)

Group	Eyes	CCL2	CCR2	LTB4	LILRA6	IL-1β	CLEC4D	S100A9	SLFN1	CD300LB
Normal group	6	1.025±0.100	1.023±0.078	1.008±0.025	1.016±0.104	1.019±0.078	1.014±0.091	0.988±0.032	1.012±0.089	1.002±0.100
PBS group	6	14.861±2.555[a]	7.687±1.642[a]	18.311±2.983[a]	4.350±0.667[a]	15.164±2.090[a]	5.077±2.143[a]	1.249±0.432[a]	5.101±1.087[a]	19.584±5.707
sEV group		5.371±1.791[ab]	3.911±1.311[ab]	10.719±2.027[ab]	4.788±1.415[ab]	9.090±2.232[ab]	4.295±1.366[a]	1.059±0.127[a]	4.313±1.637[a]	11.012±2.432
F		92.49	45.49	104.10	80.32	40.44	31.16	12.95	21.89	1.60
P		<0.01	<0.01	<0.01	<0.01	<0.01	<0.01	<0.01	<0.01	>0.01

Note: Compared with the normal group, [a]*P*<0.05; compared with the PBS group, [b]*P*<0.05 (One-way analysis of variance, Tukey test) PBS: phosphate-buffered saline; sEV: small extracellular vesicle; CCL: C-C motif chemokine; CCR: C-C motif chemokine receptor; LTB4: leukotriene B4; LILRA6: leukocyte Ig-like receptor A6; IL: interleukin; CLEC4D: C-type lectin domain family 4D; S100A9: S100 calcium binding protein A9; SLFN1: schlafen 1; CD300LB: CD300 antigen-like family member B

3 Discussion

MSC-sEVs are microvesicles less than 200 nm in diameter, secreted by MSCs, whose main functional components are exosomes. SEVs possess a lipid bilayer membrane structure with cargos of proteins and nucleic acids, functioning as intercellular bioinformation transmission mediators [12]. In this study, we investigated the reparative effects of MSC-sEVs in the early stage of retinal photoreceptor damage by establishing a mouse model of retinal light injury. The results showed that intravitreal injection of MSC-sEVs attenuated retinal structure destruction, reduced photoreceptor apoptosis, and improved retinal function. MSC-sEVs were first shown to have therapeutic effects in a myocardial ischemia-reperfusion model [13]. The beneficial effects of MSC-sEVs were then extensively validated in various systemic conditions, such as skin epithelial regeneration, cartilage tissue repair, and cerebral injury repair [7,14-15]. In ocular diseases, MSC-sEVs promote corneal epithelial damage repair, alleviate uveitis, and repair optic nerve injury [16-18]. Our previous study reported that MSC-sEVs exerted similar beneficial effects as MSCs in a mouse model of retinal laser injury [10]. In a clinical trial, MSC-sEVs promoted healing of large macular holes after vitrectomy [19]. The results of the current study confirmed the

beneficial effects of MSC-sEVs on tissue injury, especially in the treatment of retinal photoreceptors injury. Compared with MSCs, MSC-sEVs are easier to preserve and transport. Intravitreal injection of MSC-sEVs can also avoid vitreous opacity and severe immune-related reactions caused by MSC injection. The lipid bilayer membrane structure of MSC-sEVs can protect the inside cargos from degradation by enzymes with good tissue penetration, making them ideal carriers for therapeutic genes, proteins, and drugs [20]. Combined with their own beneficial effects, MSC-sEVs are expected to exert more significant effects in the treatment of ocular diseases [21].

In this study, a classic retinal light injury model was used. The main pathological changes after retinal light injury involved photoreceptor apoptosis, accompanied by retinal pigment epithelium damage [22]. This model can be used in photoreceptor injury and retinal degeneration disease research. Blue light has greater tissue penetration, causing more severe photoreceptor damage than light of other wavelengths at equal illumination. Thus, blue light is more often used in the establishment of light injury models [23-24]. In this study, blue light caused inflammation, oxidative stress reactions in the retina, and upregulation of inflammatory factor expressions. These findings provided a new direction for treatments of retinal degenerative diseases and injuries.

The results of KEGG cluster analysis showed that differentially expressed genes were mainly involved in inflammatory and immune responses. The expressions of CCL2, CCR2, LTB4, LILRA6, and IL-1β were validated by fluorescent qRT-PCR. The mRNA expression was significantly different between the sEV and PBS groups. CCL2 promoted monocyte and macrophage migration to the site of injury, IL-1β mediated immune cell activation and hyperplasia, and LTB4 was a neutrophil chemoattractant. They all played important roles in inflammatory responses [25-26]. LILRA6 is a key factor in macrophage-mediated immune responses. Downregulation of these inflammation-related factors demonstrated the role of MSC-sEVs in suppressing inflammatory responses. Intravitreal injection of MSC-sEVs has been shown to downregulate retinal CCL2 and IL-1β expression levels in both an optic nerve injury model and a retinal detachment model [18,27]. MSCs can protect skeletal muscles by downregulating LTB4 expression [28]. In addition, Hao et al. [29] reported that MSC-sEVs exerted a protective effect against bacterial inflammation-induced lung injury by upregulating LTB4. We speculated that the difference was due to the high expression of LTB4, which could recruit more neutrophils, playing an antibacterial role in bacterial inflammation. However, in nonbacterial inflammation, excessive neutrophil infiltration only causes aggravated tissue damage. In previous tumor-related studies, the effect of MSC-sEVs on the expression levels of the above factors may have been also influenced by different disease microenvironments [30]. In this study, the KEGG cluster analysis results did not implicate neuroprotective or apoptosis-related pathways. We speculated that the beneficial effect of MSC-sEVs in retinal neuroprotection was mainly achieved by inhibiting inflammatory responses.

In conclusion, the current study found a protective role of MSC-sEVs in retinal light injury. Using mRNA transcriptome sequencing analysis, we found that MSC-sEVs suppressed expression levels of multiple inflammatory factors. This study identified the mechanisms underlying the neuroprotective effects of MSC-sEVs, and provided a new research direction for the treatments of retinal injuries and retinal degenerative diseases. However, this study also had some limitations, such as the failure to determine causalities between changes in inflammatory factors and the mechanism of action of MSC-sEVs. In future studies, using interventions on upstream targets of inflammatory pathways should provide further insight into the specific mechanisms of action.

Confliction of interest None declared.

Author contribution statement Yu Bo: study design, implementation of the study, data analysis, drafting of article; Wang Kang: implementation of the study, data acquisition; Zhang Mingliang: data interpretation, data analysis; Xing Xiaoli: supervision of the study, data analysis; Li Xiaorong: conception of the study; and Zhang Xiaomin: supervision of the study, revision of article.

References

[1] Ardeljan D, Chan CC. Aging is not a disease: distinguishing age-related macular degeneration from aging[J]. Prog Retin Eye Res, 2013, 37:68-89. DOI: 10.1016/j.preteyeres.2013.07.003.

[2] Tomita H, Kotake Y, Anderson RE. Mechanism of protection from light-induced retinal degeneration by the synthetic antioxidant phenyl-N-tert-butylnitrone[J]. Invest Ophthalmol Vis Sci, 2005, 46(2):427-434. DOI: 10.1167/iovs.04-0946.

[3] Maccarone R, Di Marco S, Bisti S. Saffron supplement maintains morphology and function after exposure to damaging light in mammalian retina[J]. Invest Ophthalmol Vis Sci, 2008, 49(3):1254-1261. DOI: 10.1167/iovs.07-0438.

[4] Ghasemi M, Alizadeh E, Saei Arezoumand K, et al. Ciliary neurotrophic factor (CNTF) delivery to retina: an overview of current research advancements[J]. Artif Cells Nanomed Biotechnol, 2018, 46(8):1694-1707. DOI: 10.1080/21691401.2017.1391820.

[5] Sahu B, Leon LM, Zhang W, et al. Oxidative stress resistance 1 gene therapy retards neurodegeneration in the rd1 mutant mouse model of retinopathy[J/OL]. Invest Ophthalmol Vis Sci, 2021, 62(12):8[2022-05-06]. http://www.ncbi. nlm.nih. gov/pubmed/34505865. DOI: 10.1167/iovs.62.12.8.

[6] Shen Z, Huang W, Liu J, et al. Effects of mesenchymal stem cell-derived exosomes on autoimmune diseases[J/OL]. Front Immunol, 2021, 12:749192 [2022-05-06]. http://www.ncbi.nlm.nih.gov/pubmed/34646275. DOI: 10.3389/fimmu.2021.749192.

[7] Ha DH, Kim HK, Lee J, et al. Mesenchymal stem/stromal cell-derived exosomes for immunomodulatory therapeutics and skin regeneration[J/OL]. Cells, 2020, 9(5):1157[2022-05-10]. http://www.ncbi.nlm.nih.gov/pubmed/32392899. DOI: 10.3390/cells9051157.

[8] Guo M, Yin Z, Chen F, et al. Mesenchymal stem cell-derived exosome: a promising alternative in the therapy of Alzheimer's disease[J]. Alzheimers Res Ther, 2020, 12(1):109[2022-05-10]. http://www.ncbi.nlm.nih.gov/pubmed/32928293. DOI: 10.1186/s13195-020-00670-x.

[9] Yu B, Li XR, Zhang XM. Mesenchymal stem cell-derived extracellular vesicles as a new therapeutic strategy for ocular

diseases[J]. World J Stem Cells, 2020, 12(3):178-187. DOI: 10.4252/wjsc.v12.i3.178.

[10] Yu B, Shao H, Su C, et al. Exosomes derived from MSCs ameliorate retinal laser injury partially by inhibition of MCP-1[J/OL]. Sci Rep, 2016, 6:34562 [2022- 05-10]. http://www.ncbi.nlm.nih.gov/pubmed/27686625. DOI: 10.1038/srep34562.

[11] Zhu Y, Aredo B, Chen B, et al. Mice with a combined deficiency of superoxide dismutase 1 (Sod1), DJ-1 (Park7), and Parkin (Prkn) develop spontaneous retinal degeneration with aging[J]. Invest Ophthalmol Vis Sci, 2019, 60(12):3740-3751. DOI: 10.1167/iovs.19-27212.

[12] Zhang Y, Bi J, Huang J, et al. Exosome: a review of its classification, isolation techniques, storage, diagnostic and targeted therapy applications[J]. Int J Nanomedicine, 2020, 15:6917-6934. DOI: 10.2147/IJN.S264498.

[13] Lai RC, Arslan F, Lee MM, et al. Exosome secreted by MSC reduces myocardial ischemia/reperfusion injury[J]. Stem Cell Res, 2010, 4(3):214-222. DOI: 10.1016/j.scr.2009.12.003.

[14] Kim YG, Choi J, Kim K. Mesenchymal stem cell-derived exosomes for effective cartilage tissue repair and treatment of osteoarthritis[J/OL]. Biotechnol J, 2020, 15(12):e2000082[2022-05-16]. http://www.ncbi.nlm.nih.gov/pubmed/32559340. DOI: 10.1002/biot.202000082.

[15] Thomi G, Surbek D, Haesler V, et al. Exosomes derived from umbilical cord mesenchymal stem cells reduce microglia-mediated neuroinflammation in perinatal brain injury[J/OL]. Stem Cell Res Ther, 2019, 10(1):105[2022-05-16]. http://www.ncbi.nlm.nih.gov/pubmed/30898154. DOI: 10. 1186/s13287-019-1207-z.

[16] Samaeekia R, Rabiee B, Putra I, et al. Effect of human corneal mesenchymal stromal cell-derived exosomes on corneal epithelial wound healing[J]. Invest Ophthalmol Vis Sci, 2018, 59(12):5194-5200. DOI: 10.1167/iovs.18-24803.

[17] Li YT, Duan YN, Li H, et al. Effects of intravenous injection of human umbilical cord mesenchymal stem cells-derived small extracellular vesicles on experimental autoimmune uveitis in mice[J]. Chin J Exp Ophthalmol, 2021, 39(11):949-956. DOI: 10.3760/cma.j.cn115989-20200430-00302.

[18] Cui Y, Liu C, Huang L, et al. Protective effects of intravitreal administration of mesenchymal stem cell-derived exosomes in an experimental model of optic nerve injury[J/OL]. Exp Cell Res, 2021, 407(1):112792[2022-05-20]. http:// www.ncbi.nlm.nih.gov/pubmed/34454924. DOI: 10.1016/j.yexcr.2021.112792.

[19] Zhang X, Liu J, Yu B, et al. Effects of mesenchymal stem cells and their exosomes on the healing of large and refractory macular holes[J]. Graefe's Arch Clin Exp Ophthalmol, 2018, 256(11):2041-2052. DOI: 10.1007/s00417-018-4097-3.

[20] Zhang L, Song Y, Chen L, et al. MiR-20a-containing exosomes from umbilical cord mesenchymal stem cells alleviates liver ischemia/reperfusion injury[J]. J Cell Physiol, 2020, 235(4):3698-3710. DOI: 10.1002/jcp.29264.

[21] Lin H, Wang Y. Modification of mesenchymal stem cell derived exosomes and its application prospects in the treatment of eye disease[J]. Chin J Exp Ophthalmol, 2020, 38(10): 890-894. DOI: 10.3760/cma.j.cn115989-20200319-00186.

[22] Parver LM, Auker CR, Fine BS. Observations on monkey eyes exposed to light from an operating microscope[J]. Ophthalmology, 1983, 90(8):964-972. DOI: 10.1016/s0161-6420(83)80024-4.

[23] Shang YM, Wang GS, Sliney D, et al. White light-emitting diodes (LEDs) at domestic lighting levels and retinal injury in a rat model[J]. Environ Health Perspect, 2014, 122(3):269-276. DOI: 10.1289/ehp.1307294.

[24] Fan B, Zhang C, Chi J, et al. The molecular mechanism of retina light injury focusing on damage from short wavelength light[J/OL]. Oxid Med Cell Longev, 2022, 2022:8482149[2022-05-26]. http://www.ncbi.nlm.nih.gov/pubmed/35498134. DOI: 10.1155/2022/8482149.

[25] O'Connor T, Borsig L, Heikenwalder M. CCL2-CCR2 signaling in disease pathogenesis[J]. Endocr Metab Immune Disord Drug Targets, 2015, 15(2):105 -118. DOI: 10.2174/1871530315666150316120920.

[26] Mendiola AS, Cardona AE. The IL-1β phenomena in neuroinflammatory diseases[J]. J Neural Transm (Vienna), 2018, 125(5):781-795. DOI: 10.1007/s00702-017-1732-9.

[27] Ma M, Li B, Zhang M, et al. Therapeutic effects of mesenchymal stem cell-derived exosomes on retinal detachment[J/OL]. Exp Eye Res, 2020, 191:107899[2022-05-28]. http://www.ncbi.nlm.nih.gov/pubmed/31866431. DOI: 10.1016/j.exer.2019.107899.

[28] Su WH, Wang CJ, Fu HC, et al. Human umbilical cord mesenchymal stem cells extricate bupivacaine-impaired skeletal muscle function via mitigating neutrophil-mediated acute inflammation and protecting against fibrosis[J/OL]. Int J Mol Sci, 2019, 20(17):4312[2022-05-28]. http://www.ncbi.nlm.nih.gov/pubmed/31484417. DOI: 10.3390/ijms20174312.

[29] Hao Q, Gudapati V, Monsel A, et al. Mesenchymal stem cell-derived extracellular vesicles decrease lung injury in mice[J]. J Immunol, 2019, 203(7): 1961-1972. DOI: 10.4049/jimmunol.1801534.

[30] Shojaei S, Hashemi SM, Ghanbarian H, et al. Effect of mesenchymal stem cells-derived exosomes on tumor microenvironment: Tumor progression versus tumor suppression[J]. J Cell Physiol, 2019, 234(4):3394-3409. DOI: 10.1002/jcp.27326.